Observation of hybrid plasmon-photon modes in microwave transmission of coplanar microresonators

V. M. Muravev,[1] I. V. Andreev,[1] I. V. Kukushkin,[1] S. Schmult,[2] and W. Dietsche[2]

[1]*Institute of Solid State Physics, RAS, Chernogolovka, 142432, Russia*
[2]*Max-Planck-Institut für Festkörperforschung, Heisenbergstraße 1, D-70569 Stuttgart, Germany*

Microwave transmission of a coplanar microresonator deposited on a sample surface over a two-dimensional electron system has been studied. The transmission signal reveals a series of resonances corresponding to the excitation of hybrid cavity plasmon-photon modes, and ultrastrong plasmon-photon coupling has been realized. The hybridization frequency (Rabi frequency) is shown to be anomalously larger than the frequencies of unperturbed modes and it reaches values of up to 25 GHz. The effect of electron density and magnetic field on the excitation spectrum of cavity polariton has been investigated.

I. INTRODUCTION

For several decades, the interaction between electromagnetic radiation and matter has received considerable attention from researchers. A number of unresolved problems related to quantum electrodynamics have stimulated this interest.[1] Rabi oscillations between atomic states are observed when there is a strong coupling between an atom and the electromagnetic field of a resonator. The results of recent experiments on intersubband transitions in semiconductor microcavities reached a new limit of ultrastrong coupling, in which the Rabi frequency is comparable to the unperturbed cavity mode frequencies.[2] Recently, the unusually strong coupling between light and matter in such systems has been exploited to investigate new nonadiabatic cavity phenomena.[3] The interaction between an electromagnetic wave and a material excitation results in the formation of a compound quasiparticle called a polariton.[4] The energy of a polariton is a combination of electromagnetic energy and the intrinsic energy of the material excitation. Investigation of the coherent properties of exciton polaritons in semiconductor microresonators has revealed a number of novel research directions,[5,6] particularly, studies of long-range spatial and temporal coherences. Studies of plasmon polaritons on metal surfaces have resulted in the discovery of a whole new class of physical phenomena such as anomalous passing of light through a diffraction grating and phenomena associated with plasmon optics and metal nanosphere lasers.[7,8]

Research on plasmon polaritons in a two-dimensional electron system (2DES) has an unmatched advantage: the properties of plasmon polaritons can be tuned over wide ranges by changing the electron density of the system or by applying an external magnetic field.[9] The influence of electrodynamic effects on the plasma oscillation spectra was first theoretically investigated in the pioneering study of Stern[10] and in subsequent studies.[11–13] The theory predicts the existence of weakly damped hybrid plasmon-polariton modes in high-mobility 2DESs. These modes were first observed in experiments conducted using disk- and strip-shaped samples.[14,15] In the initial experiments, only a single polariton dispersion branch was found because of the highly radiative nature of the upper (photon) branch. In the present study, we investigate the interaction between the photon mode of the coplanar microresonator and a plasmon mode of the 2DES, which is positioned in the resonator plane at a distance that is considerably smaller that the photon wavelength. Both the polariton dispersion branches are resolved. The ultrastrong coupling between the photon and plasmon modes is investigated along with the anticrossing of their magnetodispersions. Moreover, the effects of electron density and magnetic field on the cavity polariton excitation spectrum are also studied.

II. EXPERIMENTAL TECHNIQUE

The research was executed with two 30-nm-wide AlGaAs-GaAs quantum wells (QW) structures. The quantum well is located 400 nm below the top crystal surface. The structures had electron densities $n_s = 2.1 \times 10^{11}$ and 0.97×10^{11} cm^{-2} and mobility values of 13×10^6 and 4×10^6 cm^2 V^{-1} s^{-1}, respectively ($T = 1.6$ K). A metal (Au) coplanar waveguide with a thickness of 100 nm is deposited on a crystal surface (inset of Fig. 1). The coplanar waveguide[16] is a variant of a stripline, this stripline consisted of a narrow central metal strip deposited on a GaAs-AlGaAs heterostructure substrate placed between two wide grounded electrodes. The width of the waveguide slots (W) is 30 μm, and the width of the central strip (d) is 45 μm. The parameters of the coplanar waveguide are selected such that the wave impedance is 50 Ω. Microwave radiation is guided to the structure via a coaxial cable that terminates in a microstrip transmission line. After passing through the coplanar waveguide of the sample, the microstripline, and the coaxial cable, the microwave radiation gets into the detector input. The wave impedance of the short microstripline (2 mm) is 1000 Ω, which is substantially different from 50 Ω. The coplanar microresonator includes the coplanar waveguide of length L and two identical terminating parts. Coplanar microresonators with lengths (L) of 9.5, 3.6, 2.1, and 1.0 mm are investigated. The schematic geometry of the terminating part is shown in the inset of Fig. 1. All dimensions are in micrometers. The transmission of these microresonators is measured using a Schottky diode by carrying out synchronous detection at a modulation frequency of 1 kHz. The maximum attainable Q factor of the coplanar microresonator is equal to 20. Experiments show that the Q factor is restricted mainly by the microwave losses in the structure substrate. The sample is placed in a helium cryostat

at the center of a superconducting solenoid. The experiments are carried out by applying a magnetic field perpendicular to the sample surface at $T = 1.6$ K.

III. EXPERIMENTAL RESULTS

Figure 1 shows the magnetic-field dependence of the transmission of the coplanar microresonator with a 2DES ($L = 3.6$ mm) for several values of microwave frequency. For clarity, all the curves are shifted vertically. The dashed lines indicate the signal level in the absence of input microwave power. Each curve shows a series of well-defined resonances
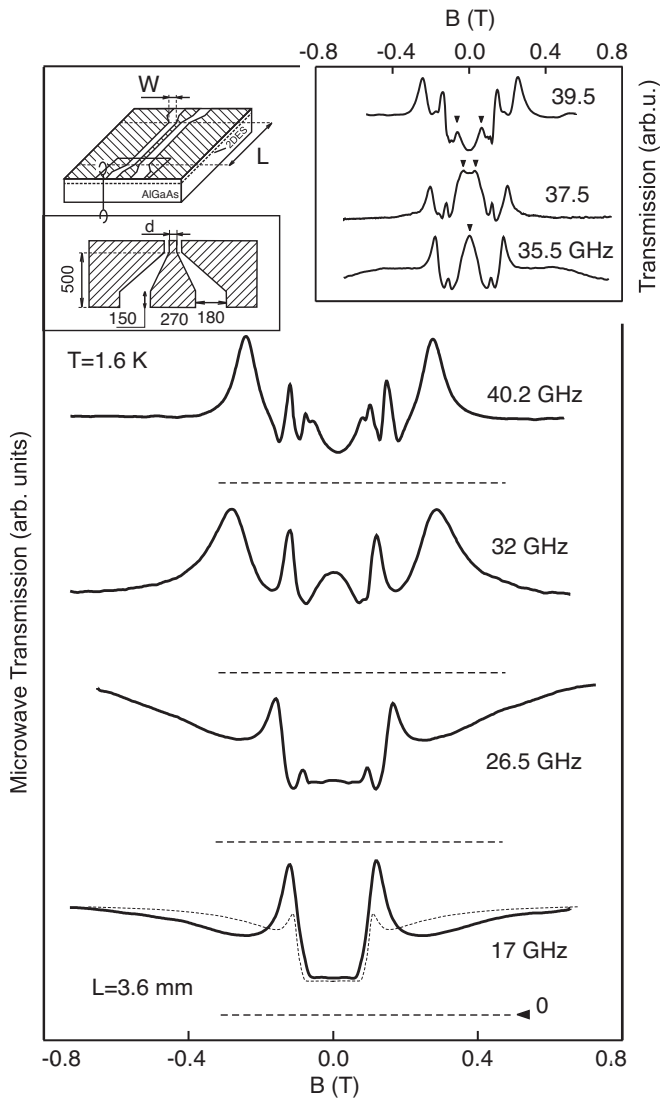
FIG. 1. Magnetic field dependencies of microwave transmission of a coplanar microresonator with 2DES measured for several microwave frequencies. For clarity, all the curves are vertically shifted. The dashed lines indicate zero signal level (in the absence of input power). The dotted curve represents the theoretical estimate of the transmission at 17 GHz. The microwave power supplied to the microstrip line is 100 nW and $T = 1.6$ K. The inset on the left shows the schematic geometry of the coplanar resonator and the one on the right shows the weak transmission resonances in small magnetic fields.
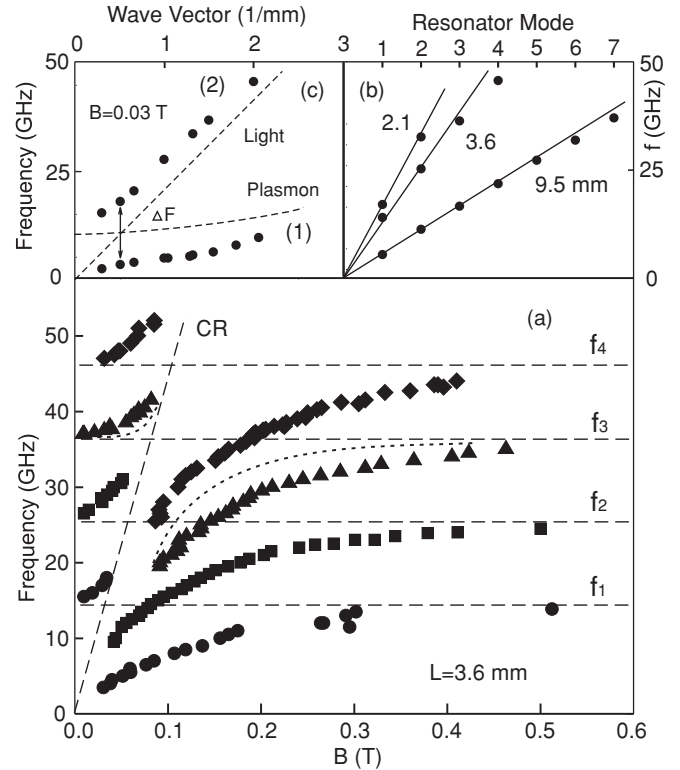
FIG. 2. (a) Dependencies of microwave resonance frequencies on magnetic fields exhibiting coplanar microresonator transmission maxima. Different symbols indicate polariton modes with different wave vectors $q = N\pi/L^*$ ($N = 1,2,3,4$) along the resonator L^* ($n_s = 2.1 \times 10^{11}$ cm^{-2}). CR is the cyclotron resonance line. (b) Coplanar cavity photon modes measured for microresonators of lengths (L) of 9.5, 3.6, and 2.1 mm. (c) Dispersion of the cavity plasmon polariton. The dispersion exhibits ultrastrong coupling and also shows that ΔF is comparable to the frequencies of unperturbed modes.

that are symmetrical with respect to zero magnetic field. It will be shown below that the resonances correspond to excitation of the hybrid photon-plasmon modes with wave vectors $q = N\pi/L$ ($N = 1,2,\ldots$) in the coplanar microresonator. Weak transmission resonances are also well defined for small magnetic fields in narrow frequency ranges (inset of Fig. 1). To gain a more detailed insight into the nature of the observed resonances, the transmission experiments were repeated for a greater number of frequencies.

Figure 2(a) shows the plots of magnetic fields of transmission maxima versus microwave frequency. The experimental points fall on four pairs of curves; in each pair one curve has a horizontal asymptote in the limit of large magnetic fields and the other approaches the same asymptote line in the limit of zero field. The horizontal asymptotes for subsequent modes are equally spaced. This indicates that the asymptotes correspond to the photon modes of the coplanar microresonator. The corresponding wave vectors are $q_N = N\pi/L^*$ ($N = 1,2,\ldots$). L^* is the effective resonator length and can be expressed as $L^* = L + 2a$, where $2a = 1.35$ mm is the span of microwelding pads and edge field corrections. To verify this hypothesis, experiments were conducted by using coplanar microresonators of different lengths. Figure 2(b)

shows the dependence of the photon mode frequencies on the microresonator mode for microresonators having different lengths with 2DES. Evidently, the difference between the frequencies corresponding to the microresonator modes is essentially dependent on L. The frequency f_N position of microresonator photon modes is expressed well by the following formula:

$$f_N = N \frac{c}{\sqrt{\varepsilon^*}} \frac{\pi}{L^*}, \quad N = 1, 2, \ldots, \quad (1)$$

where $\varepsilon^* = (\varepsilon + 1)/2$ (with GaAs permittivity $\varepsilon = 12.8$) is the effective permittivity of the coplanar resonator environment. Additional experiments performed on the samples that were similar to the ones described thus far but that had etched two-dimensional electron layers revealed a set of transmission resonances whose frequencies coincide with the values shown in Fig. 2(b), and further, these transmission resonances are independent of the magnetic field. These experiments involved a microwave frequency sweep.

An appreciable deviation of the hybrid-excitation magnetodispersion from the horizontal asymptote is observed in the vicinity of the magnetic fields corresponding to cyclotron resonance [Fig. 2(a)]. At this point, anticrossing of magnetodispersion curves of the coplanar microresonator photon modes and 2DES plasma excitations occur. These can be clarified using plots corresponding to light and magnetoplasmon dispersions [Fig. 2(c)]. Plasmon dispersion in a magnetic field B is expressed by the following formula: $\omega_p(q) = \sqrt{\omega_c^2 + \omega_0^2(q)}$, where $\omega_c = eB/m^*$ is the cyclotron frequency and $\omega_0(q)$ is the plasma excitation frequency in zero magnetic field. For the microresonator topology in this study, excited plasmons are localized in the coplanar waveguide slots and therefore have a one-dimensional nature with dispersion[17,18]

$$\omega_0^2(q) = \frac{n_s W e^2}{\pi \varepsilon_0 \varepsilon(q) m^*} q^2 \left[\ln\left(\frac{8}{qW}\right) - 0.577 \right], \quad (2)$$

where e is the electron charge, m^* is the effective mass, $2W$ is the total width of the two coplanar microresonator slots, ε_0 is the vacuum dielectric constant, and $\varepsilon(q)$ is the effective permittivity of the 2DES environment. Under our experimental conditions, normally, $\omega_c \gg \omega_0$, and as a result, the nature of plasmon dispersion is as shown by the dashed line in Fig. 2(c). The wave vector dispersion is determined by drawing a vertical line at a fixed magnetic field value on the graph shown in Fig. 2(a) and plotting the points at which the vertical line intersects the magnetodispersion curves. The corresponding wave vectors were selected according to the aforementioned rule $q = N\pi/L^*$ ($N = 1, 2, \ldots$). This procedure was repeated for all microresonators with different lengths to obtain more points on the wave-vector axis. An example, i.e., for $B = 0.03$ T, is shown in Fig. 2(c). The interaction of the plasmon and photon microresonator modes generates a hybrid excitation called a cavity polariton. Its dispersion has two branches. The photon-plasmon interaction is characterized by the repulsion of the plasmon and light dispersion curves at the intersection point ΔF. As in the case of the two-level atom interaction with the photon cavity mode, the hybridization frequency ΔF can be called the Rabi frequency.[1] The unique feature of the observed cavity plasmon polaritons is that the hybridization frequencies (Rabi

frequencies) for different modes are comparable to the mode frequencies (Fig. 2). For instance, the frequency of the first photon mode of a microresonator with L of 3.6 mm is $f_1 = 14$ GHz, whereas the Rabi splitting for this polariton mode is $\Delta F_1 = 13$ GHz. These observed frequencies of the photon modes and the Rabi splitting are characteristic of the ultrastrong coupling regime where cavity photon exchange occurs on time scales comparable to the oscillation period of light.[2,3] This is qualitatively accounted for by the fact that, in the case of cavity plasmon polaritons, the electric field of the photon resonator modes interacts with a large number of 2DES plasma electrons.

It should be noted that polariton excitation dispersion has two branches with essentially different physical properties. Branch (1) [Fig. 2(c)] is lower than the light mode and is therefore nonradiating, whereas branch (2) is radiating and its polaritons are subject to strong radiative decay. Thus, the observation of the upper branch of the plasmon polariton dispersion is a complicated experimental problem. This branch was observed for the first time in our experiments probably because the metal coplanar resonator on the sample surface prevents the radiative decay of polaritons to some extent. The presented considerations account for the low amplitude of cavity plasmon polaritons from branch 2 (inset of Fig. 1). It should be noted that a low-frequency opacity band is observed in the cavity polariton spectrum. For instance, the first mode in Fig. 2(a) is resolved only beginning with the frequency of 3.5 GHz; the second, with 9.5 GHz; and the third, with 19.7 GHz. The presence of the low-frequency opacity band is a distinctive feature of 2DES plasmon polaritons. This is explained by the fact that, in this low frequency range, hybrid excitation becomes radiative. Such radiative excitation theoretically corresponds to a mode whose field exponentially increases outward in the medium from the 2D electron layer.[19]

IV. THEORETICAL CONSIDERATIONS

The transmission of the 2DES coplanar microresonator can be estimated using the Fabry-Perot formula[20]

$$T(\omega, B) = \frac{T^2 e^{-\alpha(\omega, B)L^*}}{(1 - Re^{-\alpha(\omega, B)L^*})^2 + 4Re^{-\alpha(\omega, B)L^*} \sin^2(\varphi/2)},$$

where R and T are the reflection and transmission factors, respectively, of the coplanar resonator boundaries, $\alpha(\omega, B)$ is the absorption factor of the microresonator of effective length L^*, and φ is the change in the wave phase after the distance $2L^*$ is covered. The phase change can be determined as follows: $\varphi = 2\omega \operatorname{Re}[\sqrt{\varepsilon(\omega, B)}]L^*/c$, where $\varepsilon(\omega, B)$ is the effective permittivity of the medium where the cavity polariton propagates. Without considering coplanar waveguide topology, the effective permittivity can be estimated by the Drude approximation as half of the sum of the vacuum and 2DES permittivity values:

$$\varepsilon(\omega, B) = \frac{\varepsilon + 1}{2} \left(1 + \frac{i \, \omega_0^2 \tau}{\omega} \frac{1 - i\omega\tau}{(1 - i\omega\tau)^2 + (\omega_c\tau)^2} \right), \quad (3)$$

where τ is the elastic electron relaxation time, and ω_0 is the plasma frequency determined by using Eq. (2). Microresonator losses can be estimated as $\alpha(\omega, B) = 2\omega \operatorname{Im}[\sqrt{\varepsilon(\omega, B)}]L^*/c$.

The theoretically predicted results for microresonator transmission at 17 GHz are represented by the dotted line in Fig. 1. The dotted line in Fig. 2(a) shows the third polariton resonator mode, according to the theoretical estimate. A quantitative agreement between the theoretical and the experimental results is evident. We expect that a comprehensive theoretical description can be obtained if the geometry of the interaction between the photon microresonator mode and 2D plasma is accounted for.

V. TUNABILITY OF THE LIGHT-MATTER INTERACTION

One of the distinctive characteristics of cavity plasmon polaritons is that their spectrum can be controllably tuned over a wide range.[9] Figure 3 shows the magnetodispersion of the third polariton mode measured for two values of electron density, $n_s = 2.1 \times 10^{11}$ cm^{-2} and $n_s = 0.97 \times 10^{11}$ cm^{-2}. With decreasing two-dimensional electron density, the plasmon contribution to the hybrid cavity excitation becomes smaller, and hence the magnetodispersion appears closer to the photon dispersion line. Further, as the electron density decreases, the coupling between the photon and plasmon modes becomes weaker and results in a decrease in hybridization frequency ΔF. It follows from the theory that the Rabi frequency for the polariton mode with wave vector q_N coincides with the plasma frequency $\omega_0(q_N)$. The inset of Fig. 3 shows the dependence of the frequency ΔF on the wave mode vector for two values of the two-dimensional electron density. The dashed lines represent the theoretical dependence $\Delta F(q_N)$ determined using Eq. (2). These theoretically determined dependencies are in agreement with the experimental data. The small difference between the theoretical and experimental values may be attributed to the fact that the lateral extent of plasma excitation somewhat exceeds the total slot width $2W$.
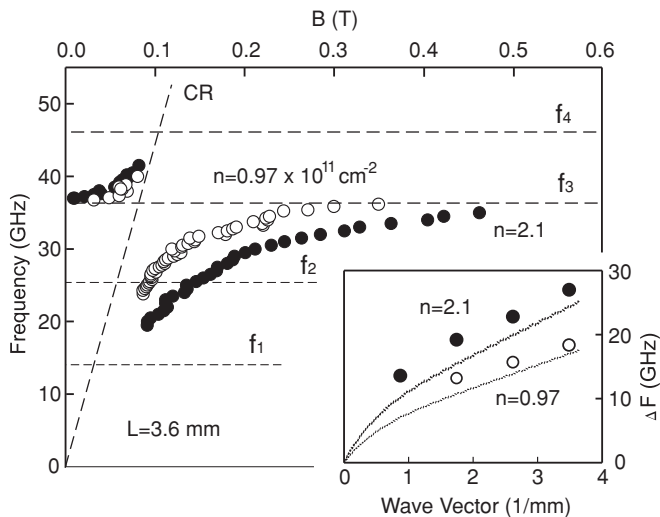
FIG. 3. Magnetodispersion of the third polariton mode measured for two values of electron density, $n_s = 2.1 \times 10^{11}$ cm^{-2} and $n_s = 0.97 \times 10^{11}$ cm^{-2} ($L = 3.6$ mm). The dashed lines indicate photon and cyclotron lines for the microresonator being studied. The inset shows the dependencies of Rabi frequency ΔF on wave vector q_N for both electron densities. The dashed lines show the theoretical results for $\Delta F(q_N)$ obtained by using Eq. (2).
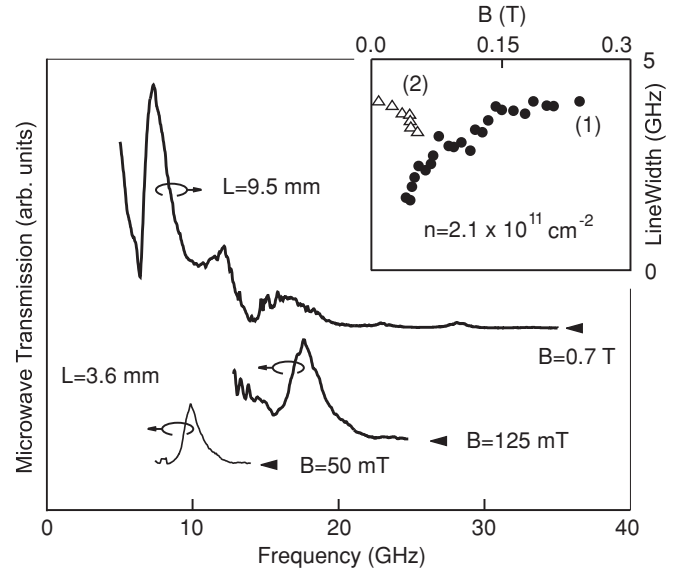
FIG. 4. Frequency dependence of microresonator ($L = 9.5$ mm) transmission measured for a strong magnetic field $B = 0.7$ T (upper curve). Frequency dependencies of transmission of a microresonator with L of 3.6 mm measured for magnetic fields $B = 125$ and 50 mT (middle and lower curves, respectively). The observed resonance corresponds to the second cavity polariton mode. The inset shows the magnetic-field dependence of the second polariton mode linewidth. (1) denotes the results corresponding to the lower dispersion branch and (2) denotes those corresponding to the upper branch.

We conclude that the Rabi frequency and the dispersion of cavity plasmon polaritons can be controlled by varying the electron density of the system.

Observation of polaritons is possible provided the time and spatial coherence conditions are fulfilled.[21] Time coherence requires the dephasing processes to be slower than the frequency of the nutation between the photon and plasmon states of cavity polaritons. For a coplanar microresonator with L of 3.6 mm, the second photon mode nutation frequency (Rabi frequency) is $\Delta F_2 = 19$ GHz [Fig. 2(a)]. The dephasing rate was estimated by measuring the resonator transmission on sweeping microwave excitation frequency (Fig. 4). The inset of Fig. 4 shows the magnetic-field dependence of the resonance width of the second cavity polariton mode. Symbol (1) denotes the points corresponding to the lower dispersion branch, and symbol (2) denotes those of the upper branch. In the limit of large magnetic fields, the microresonator photon linewidth equals $\Delta f = 4$ GHz. In our experiments, the total dephasing rate was $(\Delta f_1 + \Delta f_2)/2 \approx 6$ GHz, which is considerably less than $\Delta F_2 = 19$ GHz. Thus, the condition of ultrastrong plasmon and photon mode coupling has been experimentally realized. In order for the plasmon-photon coupling to be spatially coherent, the coherence length L_p of the plasmon must be much larger than the wavelength of light. Otherwise the dipole matrix element between plasmon and photon states that is proportional to the Rabi frequency is reduced. Detailed studies of the plasma coherence length L_p in 2DES have revealed that for the high-quality structures under investigation $L_p \approx 20$ mm.[22,23] For the microresonator with L of 3.6 mm, the wavelength corresponding to the first photon mode is 12.6 mm and that corresponding to multiple modes is less by a factor

of $N = 1, 2, \ldots$. Therefore, the spatial coherence condition is also fulfilled.

VI. CONCLUSIONS

In summary, we investigated the microwave transmission of a coplanar microresonator on a GaAs chip. The transmission signal exhibits a series of resonances corresponding to the excitation of hybrid cavity plasmon-photon modes. Ultra-strong coupling is observed in the plasmon-photon resonator mode. The Rabi frequency is shown to be anomalously large. The ratio of the experimentally observed Rabi frequency to the frequency of unperturbed modes is close to unity. The effect of electron density and magnetic field on the Rabi frequency is investigated experimentally. It is demonstrated that the hybridization frequency can be tuned over a broad range.

[1] S. Haroche and D. Kleppner, Phys. Today **42**(1), 24 (1989).

[2] D. Dini, R. Köhler, A. Tredicucci, G. Biasiol, and L. Sorba, Phys. Rev. Lett. **90**, 116401 (2003).

[3] G. Günter, A. A. Anappara, J. Hees, A. Sell, G. Biasiol, L. Sorba, S. De Liberato, C. Ciuti, A. Tredicucci, A. Leitenstorfer, and R. Huber, Nature (London) **458**, 178 (2009).

[4] K. Huang, Proc. R. Soc. London A **208**, 352 (1951).

[5] C. Weisbuch, M. Nishioka, A. Ishikawa, and Y. Arakawa, Phys. Rev. Lett. **69**, 3314 (1992).

[6] A. Kavokin and G. Malpuech, *Cavity Polaritons* (Elsevier, Amsterdam, 2003).

[7] W. L. Barnes, A. Dereux, and T. W. Ebbesen, Nature (London) **424**, 824 (2003).

[8] M. A. Noginov, G. Zhu, A. M. Belgrave, R. Bakker, V. M. Shalaev, E. E. Narimanov, S. Stout, E. Herz, T. Suteewong, and U. Wiesner, Nature (London) **460**, 1110 (2009).

[9] V. M. Muravev, A. A. Fortunatov, I. V. Kukushkin, J. H. Smet, W. Dietsche, and K. von Klitzing, Phys. Rev. Lett. **101**, 216801 (2008).

[10] F. Stern, Phys. Rev. Lett. **18**, 546 (1967).

[11] K. W. Chiu and J. J. Quinn, Phys. Rev. B **9**, 4724 (1974).

[12] V. I. Fal'ko and D. E. Khmel'nitskii, Zh. Eksp. Teor. Fiz. **95**, 1988 (1989) [Sov. Phys. JETP **68**, 1150 (1989)].

[13] S. A. Mikhailov and N. A. Savostianova, Phys. Rev. B **71**, 035320 (2005).

[14] I. V. Kukushkin, J. H. Smet, S. A. Mikhailov, D. V. Kulakovskii, K. von Klitzing, and W. Wegscheider, Phys. Rev. Lett. **90**, 156801 (2003).

[15] I. V. Kukushkin, V. M. Muravev, J. H. Smet, M. Hauser, W. Dietsche, and K. von Klitzing, Phys. Rev. B **73**, 113310 (2006).

[16] C. P. Wen, IEEE Trans. Microwave Theory Appl. **17**, 1087 (1969).

[17] I. L. Aleiner, D. Yue, and L. I. Glazman, Phys. Rev. B **51**, 13467 (1995).

[18] I. V. Kukushkin, J. H. Smet, V. A. Kovalskii, S. I. Gubarev, K. von Klitzing, and W. Wegscheider, Phys. Rev. B **72**, 161317 (2005).

[19] V. V. Popov, T. V. Teperik, and G. M. Tsymbalov, JETP Lett. **68**, 200 (1998).

[20] Y. Zhu, D. J. Gauthier, S. E. Morin, Q. Wu, H. J. Carmichael, and T. W. Mossberg, Phys. Rev. Lett. **64**, 2499 (1990).

[21] L. C. Andreani, in *Confined Electrons and Photons: New Physics and Applications*, edited by E. Burstein and C. Weisbuch (Plenum, New York, 1995), p. 57.

[22] V. M. Muravev, I. V. Kukushkin, A. L. Parakhonskii, J. H. Smet, and K. von Klitzing, JETP Lett. **83**, 246 (2006).

[23] V. M. Muravev, I. V. Andreev, I. V. Kukushkin, J. H. Smet, and K. von Klitzing, JETP Lett. **87**, 577 (2008).